Development 135, 2435-2445 (2008) doi:10.1242/dev.014704

Convergence and extension at gastrulation require a myosin IIB-dependent cortical actin network

Paul Skoglund[1,*], Ana Rolo[1,†], Xuejun Chen[2], Barry M. Gumbiner[2] and Ray Keller[1]

Force-producing convergence (narrowing) and extension (lengthening) of tissues by active intercalation of cells along the axis of convergence play a major role in axial morphogenesis during embryo development in both vertebrates and invertebrates, and failure of these processes in human embryos leads to defects including spina bifida and anencephaly. Here we use *Xenopus laevis*, a system in which the polarized cell motility that drives this active cell intercalation has been related to the development of forces that close the blastopore and elongate the body axis, to examine the role of myosin IIB in convergence and extension. We find that myosin IIB is localized in the cortex of intercalating cells, and show by morpholino knockdown that this myosin isoform is essential for the maintenance of a stereotypical, cortical actin cytoskeleton as visualized with time-lapse fluorescent confocal microscopy. We show that this actin network consists of foci or nodes connected by cables and is polarized relative to the embryonic axis, preferentially cyclically shortening and lengthening parallel to the axis of cell polarization, elongation and intercalation, and also parallel to the axis of convergence forces during gastrulation. Depletion of MHC-B results in disruption of this polarized cytoskeleton, loss of the polarized protrusive activity characteristic of intercalating cells, eventual loss of cell-cell and cell-matrix adhesion, and dose-dependent failure of blastopore closure, arguably because of failure to develop convergence forces parallel to the myosin IIB-dependent dynamics of the actin cytoskeleton. These findings bridge the gap between a molecular-scale motor protein and tissue-scale embryonic morphogenesis.

KEY WORDS: Morphogenesis, *Xenopus*, Myosin, Mesoderm, Notochord

INTRODUCTION

The tissue movements of convergence (narrowing) and extension (lengthening), often referred to as convergent extension (CE), function in many aspects of vertebrate and invertebrate morphogenesis (Keller, 2002; Keller et al., 2003; Myers et al., 2002; Zallen, 2007). Any example of CE in these diverse systems could be due to passive stretching of the tissue as a consequence of external forces, or could be active and autonomously driven by internal force-generating processes (Keller et al., 2000). CE of the *Drosophila* germband, an epithelial sheet of cells, occurs by intercalation of cells to form a narrower, longer array in a process involving apical junctional remodeling, either between pairs of neighboring cells or between multiple cells in rosettes, and is dependent on the polarized localization of myosin II in these junctions (Bertet et al., 2004; Blankenship et al., 2006; Zallen and Wieschaus, 2004). CE of the dorsal axial and paraxial mesoderm of vertebrates, a mesenchymal tissue that therefore lacks apical junctions, also occurs by the polarized intercalation of cells to form a longer, narrower array, and this process depends on a characteristic polarized protrusive activity (Glickman et al., 2003; Keller et al., 2000; Sepich et al., 2000) for which the vertebrate non-canonical Wnt/planar cell polarity (PCP) pathway is essential (Goto and Keller, 2002; Heisenberg et al., 2000; Tada and Smith, 2000). In both epithelial (Iwaki et al., 2001; Lengyel and Iwaki, 2002; Zallen and Wieschaus, 2004) and mesenchymal systems (Ninomiya et al., 2004), patterning cues in the future axis of extension are necessary for intercalation of cells in the axis of convergence. It is not known in any system how the forces that drive the active intercalation of cells, and thus CE, are actually generated and transmitted from the molecular to the cellular and tissue level. Here we examine the function of conventional myosins in this process as it occurs in the dorsal mesoderm of *Xenopus laevis*, a system in which the cellular- and tissue-level biomechanics are at least partially understood.

In *Xenopus*, active cell intercalation during CE is accompanied by a characteristic suite of polarized cell behavior [mediolateral intercalation behavior (MIB)] (Shih and Keller, 1992a), which is thought to exert traction on adjacent cells and pull them between one another. As the cells actively wedge between one another, they force the elongation of the tissue (Keller et al., 1992). At the tissue level, the axis of mediolateral intercalation, and thus the axis of tissue convergence, describes an arc across the dorsal lip of the blastopore. These convergence forces are generated by this polarized, oriented cell behavior, and are associated with the development of circumblastoporal cell intercalation leading to the shortening of these arcs of hoop stress around the blastopore, squeezing the blastopore shut, as well as driving an orthogonal anterior-posterior axial extension (Keller et al., 2000; Shih and Keller, 1992a; Shih and Keller, 1992b). These arcs of tension must run through cells and, at least at the notochord-somite boundary, through the extracellular matrix (ECM), but the molecular mechanisms and subcellular functional elements that generate or support this tension have not been identified. Disruption of the mechanical continuity of these arcs of convergence blocks the development of these circumblastoporal forces and thus blastopore closure (Keller, 1981; Schectman, 1942; Skoglund and Keller, 2007). Here we report that myosin IIB is essential for the organization of a previously undescribed cortical actin cytoskeletal network that underlies the development of these circumblastoporal convergence forces.

[1]Department of Biology, University of Virginia, Charlottesville, VA 22903, USA.
[2]Department of Cell Biology, University of Virginia, Charlottesville, VA 22903, USA.

*Author for correspondence (e-mail: frogman@virginia.edu)
†Present address: Department of Anatomy and Developmental Biology, University College London, Gower Street, London, WC1E 6BT, UK

Accepted 13 May 2008

Cytoskeletal (non-muscle) myosin II complexes are molecular motors that can both bind to and cross-link actin filaments into higher-order structures, as well as translate chemical energy into force production inside the cell by coupling ATP hydrolysis to movement along an actin filament (Geeves and Holmes, 2005; Rayment and Holden, 1994). Vertebrates have three myosin IIs (A, B and C), characterized by distinct heavy chain isoforms (MHC-A, -B and -C) (Berg et al., 2001; Golomb et al., 2004). Myosins are hexamers composed of pairs of myosin heavy chains along with two regulatory and two essential light chains to form a bivalent actin-binding unit, which further aggregates into higher-order bipolar filaments to facilitate actin cross-linking and thereby regulate cytoskeletal architecture in the cell (Landsverk and Epstein, 2005). Myosin IIA and IIB exhibit distinct biochemical rates for a conserved set of activities, including on/off rates for actin binding, rates of actin-dependent ATP hydrolysis and duty cycle characteristics governing the balance between cytoskeletal assembly activity and force production (Geeves and Holmes, 1999; Holmes and Geeves, 2000; Kelley et al., 1996). They can be differentially located even when expressed in the same cell (Kelley et al., 1996; Kolega, 1998; Maupin et al., 1994; Rochlin et al., 1995), suggesting that each isoform has specific roles.

We have investigated the role of myosin IIB in convergence and extension. In *Xenopus*, myosin IIB is the best candidate to be involved in CE because MHC-B mRNA is expressed in dorsal mesoderm and is upregulated by activin in animal cap experiments (Bhatia-Dey et al., 1993; Bhatia-Dey et al., 1998; Kelley et al., 1996), and thus is expressed at the right time and place for involvement in CE of presumptive mesoderm. We find that myosin IIB is required for normal blastopore closure by operating in the process of CE at the dorsal lip. We show that myosin IIB organizes a cortical actin network in intercalating cells, that this cytoskeletal structure is polarized with respect to the embryonic axis and that misregulation of this network is likely to underlie the range of phenotypes observed in MHC-B-depleted cells, including defects in regulation of polarized cell motility and reduced cell-cell and cell-matrix adhesion.

MATERIALS AND METHODS

Embryos and manipulations

Both pigmented and albino *Xenopus* embryos were generated by induction of egg laying and in vitro fertilization (Kintner and Melton, 1987) and staged (Nieuwkoop and Faber, 1967) by conventional means. In situ hybridizations were performed as described (Skoglund et al., 2006), using *Xho*I and SP6 RNA polymerase to make the brachyury probe from the plasmid pXBRA (Amaya et al., 1993). Explants to visualize notochordal cell behavior were cut as described in Fig. 2C.

Whole-mount immunochemistry and western blotting

MHC-A and MHC-B were detected in whole-mount staining experiments and western blotting with isoform-specific anti-peptide antibodies (Covance, Berkeley, CA). Whole-mount immunochemistry followed (Skoglund et al., 2006), using a rhodamine-conjugated anti-rabbit secondary antibody (Jackson ImmunoResearch, West Grove, PA) for confocal imaging after dehydration and clearing as described (Skoglund et al., 2006). Western blots were performed as described (Skoglund and Keller, 2007), using stage-19 embryo extracts for MHC-B and stage-13 embryos for MHC-A; extracts were run on 5% polyacrylamide gels and detection was with anti-rabbit HRP using Supersignal reagents (Pierce, Rockford, IL). Densitometry was performed as described (Skoglund et al., 2006).

Adhesion assays for C-cadherin and fibronectin and evaluation of surface expression of C-cadherin and integrin α5

The C-cadherin (C-Cad) adhesion assay was performed as described (Chen and Gumbiner, 2006; Niessen and Gumbiner, 2002), using 4 μg/ml purified recombinant C-Cad extracellular domain for coating plastic as a substrate for cells; assays were performed in triplicate with more than 400 cells per condition per experiment. The fibronectin (FN) adhesion assay was similar, but used 20 μg/ml FN as substrate (Sigma, St Louis, MO). Rescue of myosin IIB depletion-mediated adhesion to FN was with a human myosin IIB-GFP fusion construct (Vicente-Manzanares et al., 2007), injected at 100 pg per embryo at the 4-cell stage. This experiment was modified in that dorsal explants were cut at early gastrulation and cultured until stage 18, requiring addition of 10 μl of 0.5 M EDTA to facilitate dissociation to single cells but allowing visualization of fluorescent cells in the adhesion assay. The biotinylation and trypsin experiments to determine the amount of cell-surface C-Cad were as described (Chen and Gumbiner, 2006), and the same procedure was used to determine the amount of cell-surface integrin α5 using a polyclonal antibody directed against this protein.

Morpholinos and injections

A morpholino oligonucleotide (MO) directed against the translation start site of MHC-B (5′-CTTCCTGCCCTGGTCTCTGTGACAT-3′) was produced (Gene Tools, Philomath, OR); the control MO varied at five nucleotides (5′-CTTGCTCCCCTGCTCTCTCTGAGAT-3′). MO injections were into both cells at the 2-cell stage or into single blastomeres at the 32-cell stage targeted to the dorsal marginal zone by pigment cues (Lee and Gumbiner, 1995), using 0.03-5 nl of 1 mM MO to achieve 1-10 μM final concentration in the injected cell. Dorsal cells were co-injected with 0.5 nl of 30 ng/μl RNA in water in blastomeres at the 32-cell stage. C-terminal moesin-GFP was from the RNA expression plasmid CS107-GFP-Moe constructed in Dr John Wallingford's laboratory (Institute for Cellular and Molecular Biology, University of Texas, Austin, TX, USA) from the original (Litman et al., 2000). Capped RNA was made using *Asc*I/SP6 polymerase and the mMessage mMachine Kit (Ambion, Austin, TX). In some experiment, 50 ng ruby-labeled dextran (Invitrogen, Molecular Probes, Carlsbad, CA) was co-injected at the 32-cell stage. Myosins were pharmacologically targeted by injecting 50 nl of 2 mM (–)-blebbistatin (Calbiochem, San Diego, CA) in dimethylsulfoxide (DMSO; Sigma), or DMSO alone, into the blastocoel of mid-gastrula (stage 10) embryos and observing for defects in blastopore closure. Evaluating whether ectopic C-Cad expression could rescue partially MHC-IIB morphant embryos was performed in triplicate by injecting 1.5 ng C-Cad RNA (Chen and Gumbiner, 2006) with or without 5 μM MHC-IIB MO, and assaying embryos for blastopore closure defects.

Imaging

Vegetal-view movies of whole embryos were recorded on an inverted Nikon IX70 microscope running MetaMorph software and using a 4× objective. Still images were captured using either a Hamamatsu color chilled CCD or a MTI CCD camera mounted on a Zeiss stereoscope, and images processed though NIH Image (NIH), ImageJ (NIH) or Photoshop (Adobe) software. Confocal imaging used a Nikon IX70 with 60× and 100× 1.4 NA oil-immersion lenses, a BioRad Radiance2100 system and software at the Keck Center for Cellular Imaging at the University of Virginia. Framing intervals of 15 seconds to 3 minutes were used and image processing consisted of frame averaging and brightness and contrast adjustment as described previously (Shih and Keller, 1992a). Quantitation of the motion of actin foci was by plotting foci position from magnified confocal movies onto acetate sheets and then measuring anterior-posterior and mediolateral displacement (A and M, respectively) for each 1-minute interval. For notochord, ten cells with two to six foci per cell (33 foci total) were followed for 5 minutes; for pre-involution axial mesoderm [pre-notochord (PN)] and animal cap (AC), five cells with at least 20 foci were followed. The average A and M displacement in arbitrary units was generated for each cell, except for AC cells, for which it is not possible to determine anterior-posterior position, so the direction of maximum excursion of the first focus examined became M, and the orthogonal direction became A, and the average of these is presented with s.e.m.

RESULTS

Myosin heavy chain B is predominantly found in cell cortices in dorsal, axial and paraxial tissues

To examine the distribution of myosin IIB we used an isoform-specific antibody against myosin heavy chain B (MHC-B) to localize this protein complex in the developing embryo. We found

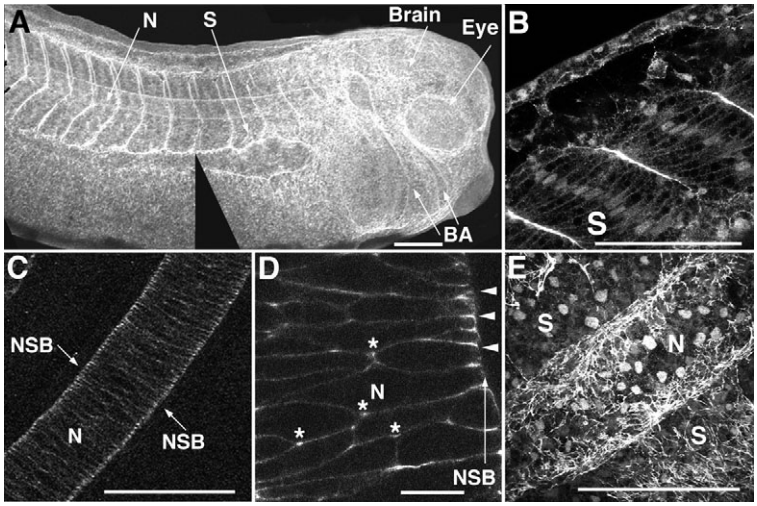

Fig. 1. Myosin IIB protein localization. (**A-C**) In tailbud-stage *Xenopus* embryos, MHC-B protein is localized to the dorsal axis (A), both at the surfaces of the somites (B) and in a polarized distribution in mature notochord (C). (**D**) Posterior notochordal cells actively undergoing convergent extension (CE) exhibit MHC-B localized to triple cell junctions inside the notochord (*), where invasive protrusions extend between adjacent cells during intercalation, and at cell-cell-matrix junctions at the notochord-somite boundary (NSB) (arrowheads). (**E**) Basal (mesodermal side) view of MHC-B staining in a deep neural-over-mesoderm explant reveals that MHC-B exhibits a fibrillar distribution over notochord and somites. BA, brachial arches; N, notochord; S, somitic mesoderm. Scale bars: 500 μm, except 50 μm in D.

that MHC-B protein is predominantly localized in the dorsal axis in tailbud-stage embryos, where it is found in the notochord and somites, as well as in the developing eye, brain and branchial arches (Fig. 1A). In confocal section, the somites of a late-neurula-stage embryo were strongly outlined, indicating that MHC-B is concentrated in somitic cell cortices that face tissue boundaries (Fig. 1B), and it could also be seen in all somitic cell cortices as well as nuclei. In the deeply interdigitated notochordal cells at the mid-axial level of a late-neurula-stage embryo, MHC-B was localized in the cell cortices and therefore outlined each cell (Fig. 1C). There was also a pronounced concentration of MHC-B protein along the surfaces of the notochordal cells where they contact the notochord-somite boundary (NSB), an ECM-rich structure that is assembled de novo during gastrulation (Shih and Keller, 1992b; Skoglund et al., 2006). In more-posterior notochordal regions, where cell intercalation and CE were still in an earlier phase, MHC-B was distributed throughout the cortical region of the cells as well, but it was also distributed in a polarized fashion within the cortex, with high levels at the anterior and posterior edges of the cells where they attach to the NSB (Fig. 1D, arrowheads), and at triple cell junctions where the large lamellipodia that lead the process of active cell intercalation are formed (Shih and Keller, 1992a) (Fig. 1D, asterisks). This pattern is consistent with a role for myosin IIB as a mechanical element in the mediolateral arcs of tension that are postulated to accompany dorsal mesodermal CE (Keller et al., 2000). Imaging the ventral surface of a neural deep-over-mesoderm explant for MHC-B revealed staining over the basal surfaces of notochordal and somitic cells (Fig. 1E), and indicated that the myosin IIB enrichment at these tissue boundaries is not due entirely to a generalized increased concentration of myosin IIB in the cortex of cells facing tissue boundaries, but also includes a component of myosin IIB organized in a linear or fibrillar pattern at these tissue boundaries.

MHC-B knockdown blocks blastopore closure and gastrulation

To examine the function of myosin IIB in the *Xenopus* embryo, we performed a morpholino oligonucleotide (MO)-mediated knockdown of MHC-B protein translation. Morphant embryos exhibited a dramatic failure of blastopore closure and gastrulation (Fig. 2A,C), which was accompanied by a reduction in MHC-B but not MHC-A protein as assayed by western blot (Fig. 2B); unilaterally morphant embryos displayed an asymmetric morphogenesis that produces an open blastopore on the injected side (Fig. 2D, right side). By contrast, embryos injected with control MO showed neither developmental defects nor a reduction in MHC-B protein levels, indicating that this failure of blastopore closure phenotype is due to loss of MHC-B (Fig. 2A,B,E). In normal embryos, the involuting marginal zone undergoes convergence and extension, which aid its involution, squeeze the blastopore shut with a closure point about two thirds of the way across the yolk plug from the dorsal lip, and extend the marginal zone tissues across the vegetal (sub-blastoporal) endoderm, thus covering it over and forming an elongated archenteron on the dorsal side of the embryo (Fig. 2F, see Movie 1 in the supplementary material). By contrast, morphant embryos failed to involute or otherwise internalize the marginal zone, failed to squeeze the blastopore shut and to cover over the endoderm and failed to elongate the dorsal body axis and form an elongate archenteron (Fig. 2G, see Movie 2 in the supplementary material). In involuting axial and paraxial mesoderm, all these processes depend on CE (Keller et al., 2000; Keller et al., 2003), and thus this phenotype is consistent with a specific failure of CE in the MHC-B MO-injected embryos. Other morphogenic processes occurred normally in morphant embryos, including cell division through the cleavage stages and the apical constriction that is associated with bottle cell formation (as revealed by the characteristic pigment accumulation; Fig. 2C,G, insets) (Hardin and Keller, 1988; Keller, 1981), indicating that they do not depend on zygotic MHC-B protein. Blastopore closure was also perturbed by acute application of the myosin II inhibitor blebbistatin to the embryo at early gastrulation stages, with 41% of embryos failing to close their blastopores and 28% exhibiting delayed blastopore closure (n=32), whereas embryos treated with DMSO alone did not exhibit significant developmental defects (5% delayed blastopore closure, n=40).

MHC-B MO-mediated failure of gastrulation is dose dependent

We titrated MHC-B MO injection to create a series of embryos with declining MHC-B protein levels. We found that the severity of failure of blastopore closure is dependent on the dose of MO injected, and thus on MHC-B levels (Fig. 2B). Unmanipulated embryos close their blastopores within 5 hours of dorsal lip formation, the normal site for closure being closer to the ventral

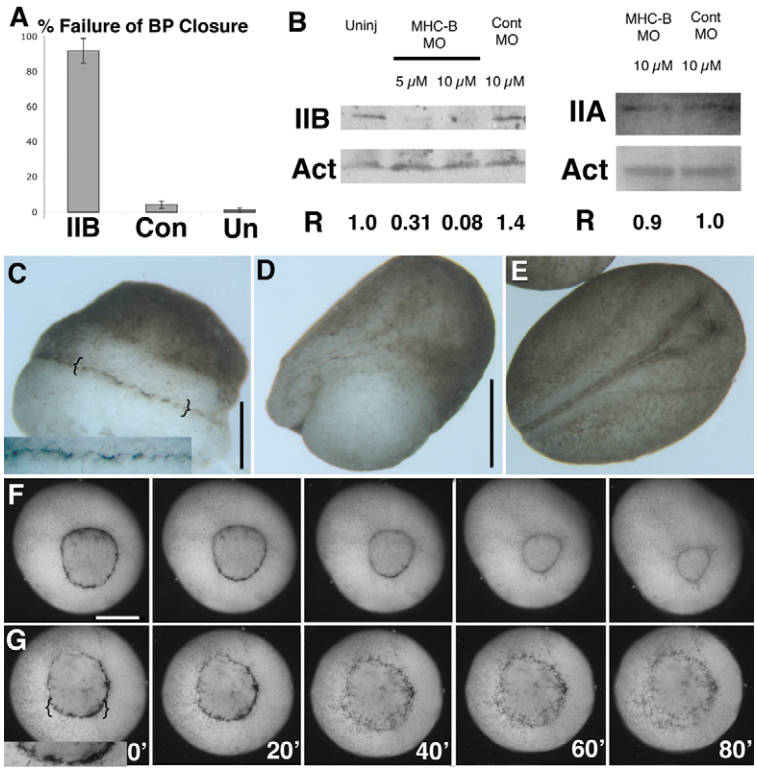

Fig. 2. Myosin IIB is required for morphogenesis at grastrulation. (**A**) Percentage of *Xenopus* embryos failing to close the blastopore plotted for 10 μM MHC-B (IIB) MO (*n*=74), 10 μM control (*n*=72) and uninjected (*n*=84) embryos, with s.e.m. (**B**) Western blots showing MHC-B (IIB), MHC-A (IIA) and actin (Act) levels in uninjected, 5 μM and 10 μM MO, and 10 μM control MO embryos. The normalized ratio of MHC-B or MHC-A to actin (R) is also shown. (**C-E**) A representative morphant embryo (C), a unilaterally (right-side) morphant embryo (D), and a control embryo (E) at stage 19. (**F**,**G**) Time-lapse movie frames showing vegetal (blastopore) view of development of a 10 μM MHC-B MO morphant (F) and a 10 μM control MO embryo (G) with time in minutes shown. Insets in C and G show bottle cells (brackets indicate regions magnified in insets). Scale bars: 500 μm, except 1 mm in D.

lip than to the dorsal lip (Fig. 3A, asterisks). By contrast, embryos injected with 2.5 μM MHC-B MO delayed blastopore closure by 2.5 hours, and exhibited a more dorsally localized closure point (Fig. 3B, asterisks). Increasing the MHC-B MO dose to 5 μM further delayed blastopore closure, which occurred in an abnormal, symmetric fashion. In some cases it failed, and a small, symmetrical blastopore remained open (Fig. 3C). At 10 μM MO, we observed the highly penetrant, large open blastopore phenotype characterized by a complete block of axial morphogenesis as described above (Fig. 3D). When the extent of notochordal extension was assayed by whole-mount in situ hybridization for the expression of brachyury (*Bra*), which identifies preinvolution mesoderm and postinvolution notochord, morphant embryos exhibited dose-dependent deficiencies in axial development, with the length of the developing notochord being inversely related to the amount of MHC-B MO injected, and were thus related to the levels of MHC-B protein in the embryo. The pattern of *Bra* expression in a normal early-neurula (stage 13) embryo reveals the normal extent of notochordal development (Fig. 3E), whereas a 5 μM MO-injected sibling embryo exhibited both delayed blastopore closure and a shorter notochord (Fig. 3F). This dose-dependent shortening of the notochord was slightly variable at 5 μM MO and these embryos often exhibited a notch or asymmetry at the dorsal lip of the blastopore (Fig. 3G); although these embryos did develop relatively normally, by the tailbud stages they exhibited a distinct dorsal bend or flexure (data not shown). By contrast, embryos injected at 10 μM MO had little or no apparent notochord, a large open blastopore and expressed *Bra* in a pattern reminiscent of that seen in normal embryos at early gastrula stages (Fig. 3H). Because the abnormal pattern of *Bra* expression in 10 μM MO morphants is similar to the normal fate map of dorsal mesoderm at the beginning of gastrulation (Keller, 1976), and because the 5 μM MO morphants exhibit *Bra* expression in an intermediate pattern, this suggests an MHC-B MO dose-dependent failure of normal cell movements to generate the dorsal axis at gastrulation, rather than a failure of tissue specification.

MHC-B-depleted cells show loss of polarity and loss of adhesion

To examine the cellular response to depletion of MHC-B, we generated mosaic embryos by injecting MHC-B MO into one dorsal cell at the 32-cell stage. Normally, internal notochord cells are bipolar, with large lamelliform protrusions on both medial and lateral ends. As cell intercalation proceeds, and internal cells intercalate into the boundary row of cells, they may undergo a short period of blebbing at the boundary, but they quickly become quiescent and form a flattened surface on the boundary, with protrusive activity apparently inhibited by contact with the boundary (Shih and Keller, 1992b). This 'boundary capture' stabilizes and defines notochordal separation from the somitic mesoderm (Keller and Danilchik, 1988; Shih and Keller, 1992b). When embryos mosaic for 10 μM MHC-B MO were examined, most morphant cells were excluded from the otherwise normal embryo by late gastrula stages, apparently owing to their relatively low adhesion (see below; data not shown). Reducing the concentration of MO injected to 5 μM leads to embryos mosaic for partially MHC-B-depleted cells that remain in the notochord until neurula stages, and these cells can be imaged during morphogenesis in dorsal, axial explants in which the endodermal epithelium covering the notochord is removed (Fig. 4A). In these partially MHC-B-depleted cells, protrusive activity was upregulated at the ends of cells that bound the NSB. These protrusions were abnormally large, superficially resembling blebs exhibited by dying cells. However, unlike blebs, which are hemispherical, these protrusions adopted whatever shape the space

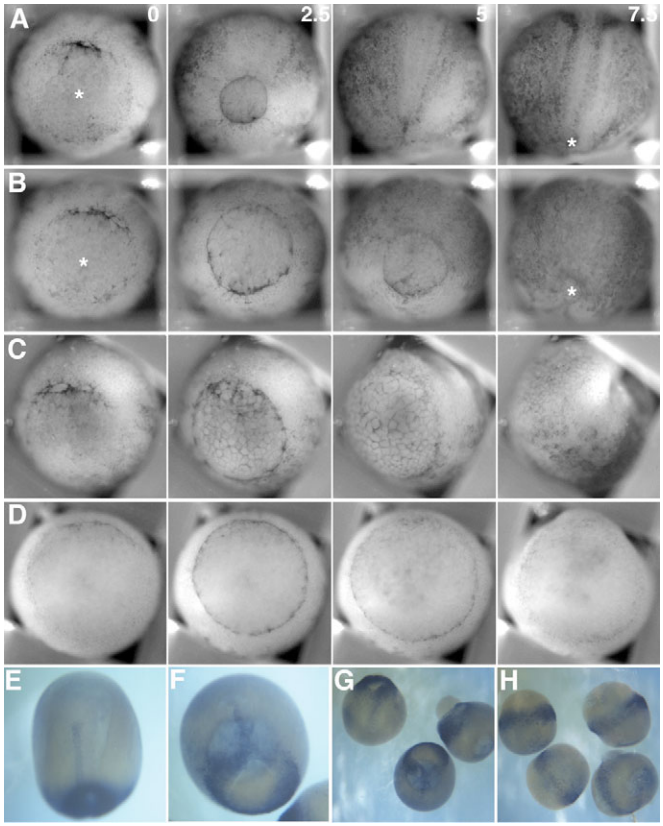

Fig. 3. Myosin IIB MO-mediated failure of gastrulation is dose dependent. (**A-D**) Still images from simultaneous time-lapse videorecordings showing vegetal views of control (A) and morphant *Xenopus* embryos injected with 2.5 μM (B), 5 μM (C) and 10 μM (D) MHC-B MO. Embryos are oriented with their dorsal side up. At stage 10 (*t*=0), bottle cells form in the dorsal lip of the blastopore of all control and morphant embryos. By control stage 12 (*t*=2.5), ventral bottle cells have formed in all control and morphant embryos, but blastopore closure is delayed in a MHC-B MO dose-dependent manner. The site of blastopore closure in 2.5 μM (B, *t*=7.5) morphant embryos is not located as ventrally as in control embryos (A, *t*=7.5). Asterisks indicate the center of the yolk plug at *t*=0 and the point of blastopore closure at *t*=7.5. (**E-H**) RNA in situ hybridizations of stage-13 embryos for brachyury expression reveals the extent of notochordal morphogenesis in a control embryo (E), and reduced notochordal morphogenesis in a 5 μM morphant (F). The 5 μM morphant embryos exhibit some variability in notochordal extension (G), but 10 μM morphant embryos essentially lack notochord extension (H).

around the cells allowed and so they were variably loboform, lamelliform and circuitously channeled between other cells (Fig. 4B, see Movie 3 in the supplementary material). Partially morphant cells were eventually shed from the notochord. Although they often fragmented similar to myosin-null *Dictyostelium* cells in mechanically restricted environments (Laevsky and Knecht, 2003), the partially morphant cells continued to exhibit cell motile behaviors in culture for more than 5 hours after shedding, indicating that they are not necrotic (data not shown). Just before being shed, the internal ends of these morphant cells were the last part of the cell to adopt this behavior and, on doing so, the cells left the notochord to take up residence in whatever space was available

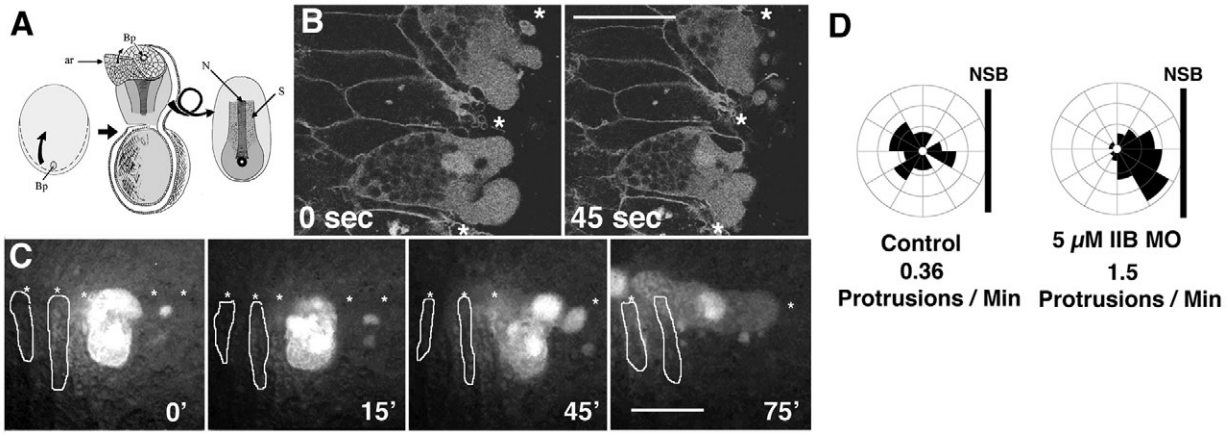

Fig. 4. Partially myosin IIB-depleted notochordal cells exhibit polarization and adhesion phenotypes. (**A**) Explanting the dorsal tissues of a *Xenopus* embryo neurula above the blastopore (Bp) and removing the endodermal archenteron roof (ar) exposes the notochord (N) and somitic mesoderm (S) for imaging during CE. (**B**) In such explants, confocal time-lapse imaging of a notochord mosaic for cells injected with 5 μM MHC-B MO reveals that morphant cells (labeled), in the background of a notochord expressing a membrane-bound GFP (revealing cell outlines), exhibit loss of regulation of polarized cell motility. Asterisks, NSB. (**C**) An epifluorescent time-lapse sequence of one partially morphant labeled cell shows that it exhibits loss of regulation of polarized cell motility and eventually is excluded from the notochord (cell outlines are normal notochordal cells in this mosaic explant). (**D**) Control notochordal cells at or near the NSB exhibit monopolar motile behaviors, with few protrusions toward the NSB, whereas 5 μM MO morphant cells express increased motility and improperly direct this motility towards the boundary. One unit represents 6% of the total protrusive activity directed towards that sector, and each sector is oriented relative to the NSB. Scale bars: 50 μm.

to them, which was usually the groove formed at the NSB (Fig. 4C, see Movie 4 in the supplementary material). This phenotype represents both an increase in protrusive activity and an abnormal distribution of protrusive activity, and indicates a polarization defect in these cells (Fig. 4D). These behaviors suggest a loss of cortical mechanical integrity, loss of the normal boundary-mediated constraint on protrusive activity, loss of cell adhesion to the boundary ECM, and loss of cell-cell adhesion in morphant cells.

The cortical actin cytoskeleton is polarized relative to the embryonic axis in notochordal cells

We have visualized the F-actin cytoskeleton in live notochordal cells using the F-actin-binding probe moesin-GFP and laser-scanning confocal microscopy. Normal, non-morphant notochordal cells display a dynamic, basket-like network of fine, straight actin bundles organized in a hub-and-spoke fashion, with several hubs or foci where actin bundles meet arrayed across the cortical region of these elongate cells (Fig. 5A, see Movie 5 in the supplementary material). During notochordal intercalation, these foci are dynamic, constantly moving within the cell on a timescale of seconds. The predominant displacement of these foci, and thus of the actin cables attached to them, is parallel to the long axis of these cells (Fig. 5B,C). Because the anisotropic behavior of these cytoskeletal elements in notochordal cells corresponds to both the axis of mediolateral cell intercalation and the axis of convergence, this is consistent with a role for the cortical actin network in notochordal cell intercalation. Examining this cortical actin network in pre-involution mesoderm revealed that it is less robustly polarized, and in animal cap cells it is not polarized, indicating that it becomes polarized with the same developmental time-course as exhibited by cell intercalation behaviors (Fig. 5C).

MHC-B-depleted cells show dose-dependent loss of cortical actin cytoskeletal integrity

We wished to determine whether myosin IIB regulates the cortical actin network in notochordal cells. We found that in notochordal cells morphant for MHC-B MO at a dose of 5 μM, the cortical actin network is perturbed, indicating that the proper regulation of this network requires myosin IIB in these cells (Fig. 5D, see Movie 6 in the supplementary material). During this behavior, actin cables were absent or few in number, and those that were present were thickened and sinuous. Moreover, the cells appeared able to make large, rapidly extending protrusions but could not retract them or effectively pull the cell body toward the protrusions. The transition between normal and perturbed cortical actin organization in morphant cells correlated with the loss of the normal, polarized protrusive activity of the notochord cells and the eventual exclusion of MHC-B-depleted cells from the notochord (Fig. 5E, see Movie 7 in the supplementary material). This change in protrusive activity was accompanied, or closely followed, by disruption of the characteristic hub-and-cable pattern of cortical actin microfilament bundles. Instead of foci connected by straight (and thus apparently taut or tensioned) actin cables, there were fewer, thicker cables that were often sinuous, unconnected to foci and appeared to be under little or no tension. These observations suggest that the normal foci-cable array of cortical actin cytoskeleton depends on myosin IIB.

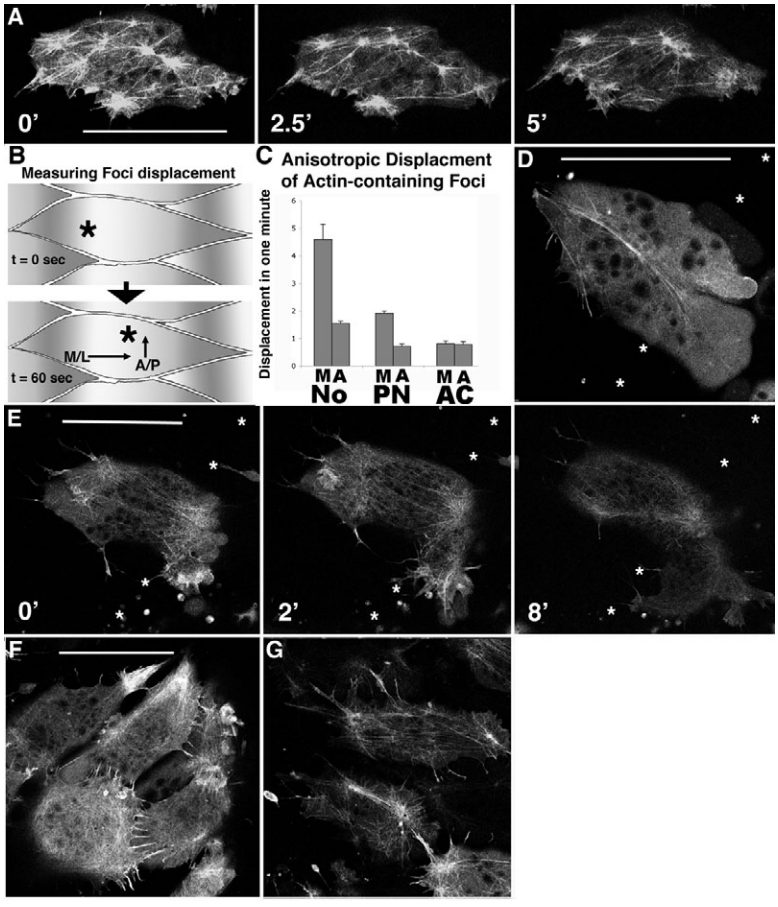

Fig. 5. Partially myosin IIB-depleted notochordal cells exhibit a cortical actin phenotype. (**A**) Confocal microscopy of *Xenopus* notochordal control cells injected with moesin-GFP reveals a dynamic cortical actin network in a basket-like distribution, with 3-5 foci of actin visible per cell. (**B**) These actin-rich foci (asterisk) visibly move within the cell on a sub-minute timescale. (**C**) Plotting the relative displacement of foci along the embryonic axis in the mediolateral (M) and anterior-posterior (A) directions, reveals that the rate of displacement of these foci is greater in the mediolateral dimension than in the anterior-posterior dimension for notochordal cells (No) ($P<0.02$ by Student's *t*-test), and this polarity is also detectable in pre-notochordal cells (PN) but not in animal cap cells (AC). (**D**) In contrast to control cells, MHC-B MO-injected cells exhibit dramatic disruption of the cortical actin network. Asterisks (also in E) indicate the NSB. (**E**) Confocal time-lapse sequence of a morphant cell exhibiting aberrant motility concomitant with cortical actin breakdown. Elapsed time is shown in minutes. (**F**,**G**) Mildly morphant notochordal cells (1 μM MO) remain in the notochord with intact cortical actin networks, but exhibit profuse filopodia (F) as compared with control notochordal cells (G), revealing a threshold cell polarity phenotype in response to MHC-B depletion. Scale bars: 50 μm.

Both the disruption of the cortical actin cytoskeleton and the cellular exclusion phenotype are dependent on MHC-B levels, as morphant notochordal cells with a low-level MHC-B depletion (1 μM MO) both remained in the notochord and had a relatively intact cortical actin cytoskeleton (Fig. 5F,G, see Movie 8 in the supplementary material). However, these morphant cells had more actin-rich filopodial protrusions than normal cells, indicating that the polarized protrusive activity characterizing these intercalating cells is sensitive to MHC-B levels.

Adhesion of morphant cells to cadherins and to fibronectin matrix is reduced

Perturbing myosin II function affects cell adhesion and cadherin localization in mice, *Drosophila*, *Dictyostelium* and cultured cells (Conti et al., 2004; Shewan et al., 2005; Xu et al., 1996). Because regulation of C-cadherin (C-Cad) is necessary for mesodermal CE in *Xenopus* embryos (Brieher and Gumbiner, 1994; Lee and Gumbiner, 1995; Zhong et al., 1999), we assayed C-Cad-mediated adhesion in MHC-B-depleted cells. We found a dramatic dose-dependent reduction in adhesion (Fig. 6A). However, morphant cells maintained their cell-surface C-Cad protein levels when assayed by trypsin digestion (Fig. 6B) or surface biotinylation (data not shown). Because expressing exogenous C-Cad protein did not rescue the blastopore closure phenotype of partially morphant embryos, but rather made this phenotype worse, this again suggests that C-Cad protein levels are not limiting in morphant embryos (Fig. 6E). Morphant cells also exhibited a reduction in adhesion to fibronectin (FN) (Fig. 6C), indicating that integrin-receptor-mediated adhesion is dependent on myosin IIB in these cells. Similar to what was observed for C-Cad, morphant cells maintain their cell-surface integrin α5 protein levels when assayed by trypsin digestion (Fig. 6D) or surface biotinylation (data not shown). Expression of a human myosin IIB heavy chain-GFP fusion rescued FN adhesion in morphant cells (Fig. 6F), indicating that the MO specifically targets the myosin IIB heavy chain. Thus, myosin IIB is necessary for both cell-cell and cell-matrix adhesion, either directly or indirectly through its role in organizing the cortical actin network, as the assembly state of actin affects cadherin function (Jaffe et al., 1990).

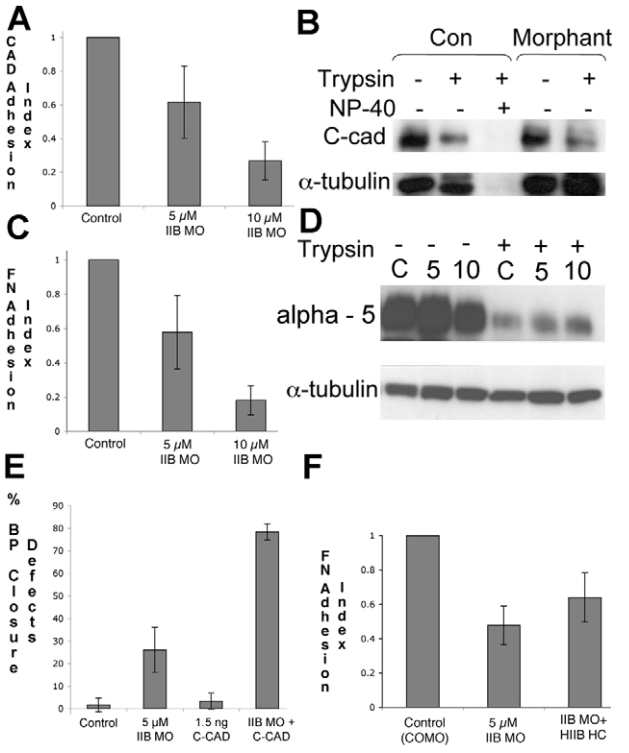

Fig. 6. Cell-cell and cell-matrix adhesion are affected in morphant cells. (**A**) Morphant dorsal axial cells at stage 13 exhibit a dramatic dose-dependent reduction in adhesion to recombinant extracellular domain of C-cadherin (C-Cad). (**B**) However, cell-surface levels of C-Cad are unchanged in morphant cells, as similar levels of control and morphant cell C-Cad is available on the cell surface for trypsin digestion. (**C**) Morphant cells also show a dramatic reduction in adhesion to fibronectin (FN). (**D**) Cell-surface levels of integrin α5 are not affected by myosin IIB depletion. (**E**) Failure of blastopore closure due to MHC-B depletion is not rescued by exogenous expression of C-Cad, consistent with the hypothesis that C-Cad levels are not limiting in morphant embryos. (**F**) Adhesion to FN in morphant cells is rescued by co-expression of exogenous human MHC-B.

DISCUSSION

MHC-B plays an important and necessary role in CE

Several observations suggest that myosin IIB is involved in CE. First, MHC-B mRNA is expressed in the dorsal mesoderm of the embryo and is upregulated by activin treatment of animal caps, which also induces CE in these caps (Bhatia-Dey et al., 1998; Kelley et al., 1996). Second, we find MHC-B protein distributed in a polarized fashion in notochordal cells undergoing CE. Third, we show that reducing MHC-B protein in the embryo leads to the failure of gastrulation. We find that myosin IIB organizes a polarized cortical actin network in notochordal cells, and that this network is required for CE. Because this network is required for both polarized expression of cell motility and regulation of cell adhesion, these defects are likely to be responsible for the failure of morphogenesis. This work identifies the dynamic, myosin IIB-dependent cortical actin network as the cell component integrating adhesion and polarized motility during CE.

In *Drosophila*, myosin II is also involved in the epithelial cell intercalation that occurs during germ band CE (Bertet et al., 2004; Zallen and Wieschaus, 2004). Cell intercalation in germ band extension involves remodeling of the circumapical adherens junctions during neighbor changes among pairs of cells (Bertet et al., 2004) or in multicellular rosettes of cells (Blankenship et al., 2006), whereas the cell intercalation in the *Xenopus* dorsal mesoderm involves deep, non-epithelial mesenchymal cells, which are attached to each other at foci and lack an apical junctional complex. In *Xenopus*, we find myosin IIB distributed cortically in involuting mesodermal cells, with higher medial and lateral concentrations, whereas in the *Drosophila* germ band myosin II is localized asymmetrically adjacent to anterior and posterior apical contacts (Bertet et al., 2004; Zallen and Wieschaus, 2004), indicating that although these two examples of CE both use myosin II, they are mechanistically distinct processes.

Embryos morphant for MHC-B fail to close their blastopores in a fashion that indicates failure of CE in the involuting dorsal axial and paraxial mesoderm (Keller et al., 2000; Keller et al., 2003). Normally, CE of the axial and paraxial mesoderm constricts the involuting marginal zone, which closes the blastopore, and simultaneously elongates the body axis by extension. This occurs because the polarized protrusive activity and traction of the deep mesodermal cells, the resulting cell intercalation, and the consequent convergence, all occur along the presumptive mediolateral axis of the dorsal tissues, which in the involuting marginal zone of the

embryo is described as an arc-like pattern around the blastopore (Keller et al., 1992; Keller, 1984; Shih and Keller, 1992b). Shortening these arcs by cell intercalation results in constriction of the blastopore and the resulting extension in the perpendicular direction results in axial elongation, all in one stroke (Keller et al., 2003; Keller and Shook, 2004). Morphant embryos show a dose-dependent gradation of success in constricting the blastopore, with stronger depletions failing entirely and weaker depletions showing limited closures and specific defects in dorsal, axial extension. This behavior is strong evidence for the myosin IIB dependence of CE. By contrast, other morphogenic processes occur normally, including cell division during cleavage and bottle cell formation, suggesting that the cellular mechanisms underlying CE in dorsal mesodermal tissue are those most dependent on myosin IIB, consistent with a morpho-mechanical role for this myosin isoform in CE.

Cellular MHC-B morphant phenotypes show that MHC-B is essential for a specialized cortical actin cytoskeleton necessary for the development of convergence forces

Protrusive activity of the type displayed in a bipolar, oriented fashion by the deep mesodermal cells is invariably associated with traction forces in cell culture on deformable substrates (Beningo and Wang, 2002; Harris et al., 1980; Lo et al., 2004; Lo et al., 2000). This suggests that these cells are exerting traction on adjacent cells or on the matrix and are under tension in the mediolateral axis, which is also the axis of convergence. Notochordal cell elongation and intercalation in the presence – and only in the presence – of their characteristic bipolar protrusive activity further supports this contention. What generates the tensile forces at the cell level that drives cell intercalation and convergence and what integrates these forces over long distances along the arcs of convergence are long-standing questions. The anisotropic dynamic behavior of the cortical actin cytoskeleton described here and its perturbation in myosin IIB morphant cells suggest that this cytoskeletal architecture and associated cortical tension play a large role in this process. First, the predominant movement of the actin nodes, and thus the predominant change in length of the actin cables connecting them, is in the mediolateral axis. This is also the axis of cell intercalation, cell traction generation and tensile force generation, suggesting that this cytoskeleton functions in these processes. These tensile forces across the involuting marginal zone rise to 1.5 μN during gastrulation (D. Shook, personal communication). Second, the sequence of defects appearing in cells partially depleted for MHC-B include loss of integrity of this cortical actin network, abnormal protrusive activity, loss of the elongate polarized morphology, apparent loss of cortical integrity as judged by the inability of the cell to maintain its shape, accommodating instead to surrounding spaces, and, finally, the loss of adhesion. Third, myosin IIB is localized to the cell cortex, which is expected to be under tension along cell surfaces between protrusions (Kolega, 1986), and is thus important in developing mediolateral traction or resisting the cell elongation it might produce. Myosin IIB is also concentrated in the cell-cell, cell-matrix junctions of cell surfaces facing the mesodermal NSB boundary, a region of stable anchorage and suppression of protrusive activity that is required for the integrity of the boundary and for directed extension (Shih and Keller, 1992b; Skoglund et al., 2006; Skoglund and Keller, 2007). Myosin IIB levels are also elevated at triple cell junctions found in the interior of the notochord, an increase that probably reflects the presence of the polarized, medial and lateral protrusions thought to generate the traction for cell intercalation. Finally, the vigorous but aberrant protrusive activity, the inability to constrain their shape in a mechanically resistant environment, and the tendency for fragmentation are all characteristics that myosin IIB morphant *Xenopus* cells have in common with myosin II-null mutants in *Dictyostelium*, in which this molecule functions principally as an actin cross-linker and is important in the maintenance of cortical integrity necessary for migration along mechanically restricted environments (Laevsky and Knecht, 2001; Laevsky and Knecht, 2003; Xu et al., 2001). These data combine to suggest that myosin IIB has a mechanical role in the generation or transmission of the mediolateral tensile forces thought to underlie CE, and thereby blastopore closure and axial elongation (Keller et al., 2000).

Myosin IIB is essential for cell-cell and cell-matrix adhesion

Severely depleted morphant cells eventually appear to lose adhesion to adjacent cells and ECM, a loss of adhesive ability that was confirmed by decreased adhesion to defined cadherin and FN substrates. This suggests a role for myosin IIB in adhesion, a notion supported by the fact that myosin IIB is important for clustering E-cadherin at adhesion sites and for forming adhesions in cultured epithelial cells (Shewan et al., 2005). In these mesenchymal *Xenopus* cells, the important cadherin in CE appears to be C-cad (Brieher and Gumbiner, 1994; Zhong et al., 1999), and we that show myosin IIB regulates *Xenopus* cell-cell adhesion by a mechanism distinct from regulating the surface expression of C-cad. The fact that both cadherin-mediated adhesion to cadherin and integrin-mediated adhesion to ECM are affected in morphant cells suggests a general and perhaps indirect effect of myosin on adhesion. This consequence of myosin IIB depletion might be mediated by loss of the actin cytoskeletal organization, as it parallels the loss of adhesion that occurs upon disruption of microfilaments with cytochalasin (Jaffe et al., 1990), and suggests that a normal function of the dynamic cortical actin network is to dynamically regulate cell-cell and cell-matrix adhesion on notochordal cells in a manner appropriate to support CE.

Both integrin (O'Toole et al., 1994) and cadherin (Marsden and DeSimone, 2003) adhesive functions can be modulated by cytoplasmic signals, and modulation of one of these adhesion systems can affect the other (Finnemann et al., 1995; Winklbauer, 1998). Our results allow for the possibility that this interdependency could be partially mediated by local modifications of the cortical actin network, because we show that both adhesion systems depend on this network. This view is supported by the observation that *Xenopus* C-Cad intracellular tail interactions with p120 catenin regulate the local pattern and density of the cortical actin network in blastomeres (Tao et al., 2007).

Summary of myosin IIB function in CE

A summary of how we think myosin IIB functions in the context of what is known about CE in *Xenopus* is shown in Fig. 7. The mediolateral intercalation of cells occurs as the initially unpolarized, isodiametric deep mesodermal cells become polarized to form large filo-lamelliform protrusions at their medial and lateral ends, which display repeated cycles of extension (Fig. 7A, black arrows) and shortening (Fig. 7A, gray arrows) (Keller et al., 1989; Shih and Keller, 1992a). As this type of protrusive activity is invariably associated with exertion of traction on the substrate (Beningo et al., 2002; Harris et al., 1980; Lo et al., 2004; Lo et al., 2000), which in this case is either adjacent cells or ECM, this protrusive activity is very likely to generate the traction that first elongates the cells and then pulls them between one another, thus

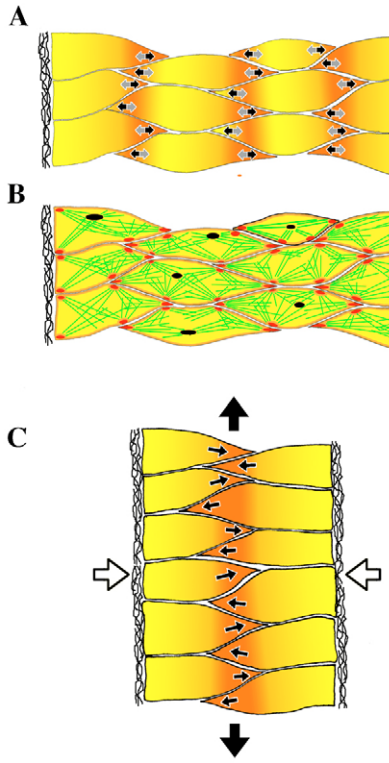

Fig. 7. A myosin IIB-dependent cortical actin network functions to integrate cell adhesion and polarization to generate directed forces driving morphogenesis. (**A**) Cell intercalation in the *Xenopus* notochord requires two distinct cell activities: cell contraction in the cell body (gray arrows) and polarized protrusive activity (black arrows). (**B**) Contraction events are driven by the myosin IIB-dependent cortical actin network (green lines), which is organized into dynamic foci (black) and interacts with myosin IIB at adhesion sites (red). (**C**) Integrating this episodic cell shortening with polarized protrusive activity and dynamically regulated myosin IIB-dependent adhesion leads to cell intercalation (white arrows) and tissue-level convergence and extension (large black arrows). The deeply interdigitated notochordal cells at this stage have adopted a monopolar protrusive activity (small black arrows). The extracellular matrix of the NSB is lateral in each case.

directly shortening the mediolateral axis of the tissue and, indirectly, by wedging the cells between one another, extending the anterior-posterior axis (Fig. 7C, large arrows). The myosin IIB-dependent dynamic cortical actin network consisting of actin cables (Fig. 7B, green) meeting at foci or nodes (Fig. 7B, black) serves as a tensile element in the cell cortex that limits the elongation of the cell, driven by the polarized traction, and transmits the tension from one adhesion site to another inside the cell. Tension is transmitted from cell to cell through adhesion sites, generating arcs of tension across the tissue fabric. The dynamic oscillation of the length of the actin cables and movement of the nodes is along the mediolateral axis, which is also the axis of development of the convergence forces and suggests an active contractile role for the cortical actin network in CE. The cortical distribution of myosin IIB and the apparent lack of cortical tension in the morphant cells are consistent with involvement of this molecule in cross-linking the cortical actin cytoskeleton. In addition to maintaining cortical integrity, myosin IIB might also participate in active contraction by reeling actin filaments into the foci and thus generating the force for intercalation, but this remains to be determined by imaging these molecules and assaying their activity state in living cells. The concentration of myosin IIB in the anterior/posterior corners of the cell surfaces contacting the ECM structure at the NSBs (Fig. 7B, red) might reflect a mechanical reinforcement at this critical boundary. The apparent concentration at the interior, triple cell junctions (Fig. 7B, red) might reflect the same thing, although in this case the increased staining may not reflect an increase in myosin IIB per unit area of cortex, but instead the close apposition of four cortical regions or the presence of the molecule in the lamellipodia at these ends of the cells. In either case, it reflects a high concentration of myosin IIB per cell volume, which again may reflect a mechanical reinforcement. Myosin IIB is involved in polarized cell behavior (Lo et al., 2004), but whether its involvement is direct or is mediated by its role in organizing the actin cytoskeleton remains to be determined.

We thank Ammasi Periasamy and Ye Chen for help with confocal imaging at the Keck Center for Cellular Imaging (KCCI) at the University of Virginia; Lance Davidson, Caroline Flournoy, Crystal Scott and David Shook for stimulating discussions in the laboratory, both with reference to possible molecular mechanisms and to imaging techniques; and Miguel Vincente-Manzanares and Rick Horowitz for the myosin IIB-GFP fusion plasmid. This work was supported by National Institutes of Health (NIH) grants HD36426-01 and HD25594-13 to R.K. and a predoctoral fellowship from Fundação para a Ciência e a Tecnologia (FCT) SFRH/BD/4851/2001 to A.R.

Supplementary material

Supplementary material for this article is available at
http://dev.biologists.org/cgi/content/full/135/14/2435/DC1

References

Amaya, E., Stein, P. A., Musci, T. J. and Kirschner, M. W. (1993). FGF signalling in the early specification of mesoderm in Xenopus. *Development* **118**, 477-487.
Beningo, K. A. and Wang, Y. L. (2002). Flexible substrata for the detection of cellular traction forces. *Trends Cell Biol.* **12**, 79-84.
Beningo, K. A., Lo, C. M. and Wang, Y. L. (2002). Flexible polyacrylamide substrata for the analysis of mechanical interactions at cell-substratum adhesions. *Methods Cell Biol.* **69**, 325-339.
Berg, J. S., Powell, B. C. and Cheney, R. E. (2001). A millennial myosin census. *Mol. Biol. Cell* **12**, 780-794.
Bertet, C., Sulak, L. and Lecuit, T. (2004). Myosin-dependent junction remodelling controls planar cell intercalation and axis elongation. *Nature* **429**, 667-671.
Bhatia-Dey, N., Adelstein, R. S. and Dawid, I. B. (1993). Cloning of the cDNA encoding a myosin heavy chain B isoform of Xenopus nonmuscle myosin with an insert in the head region. *Proc. Natl. Acad. Sci. USA* **90**, 2856-2859.
Bhatia-Dey, N., Taira, M., Conti, M. A., Nooruddin, H. and Adelstein, R. S. (1998). Differential expression of non-muscle myosin heavy chain genes during Xenopus embryogenesis. *Mech. Dev.* **78**, 33-36.
Blankenship, J. T., Backovic, S. T., Sanny, J. S., Weitz, O. and Zallen, J. A. (2006). Multicellular rosette formation links planar cell polarity to tissue morphogenesis. *Dev. Cell* **11**, 459-470.
Brieher, W. M. and Gumbiner, B. M. (1994). Regulation of C-cadherin function during activin induced morphogenesis of Xenopus animal caps. *J. Cell Biol.* **126**, 519-527.
Chen, X. and Gumbiner, B. M. (2006). Paraxial protocadherin mediates cell sorting and tissue morphogenesis by regulating C-cadherin adhesion activity. *J. Cell Biol.* **174**, 301-313.
Conti, M. A., Even-Ram, S., Liu, C., Yamada, K. M. and Adelstein, R. S. (2004). Defects in cell adhesion and the visceral endoderm following ablation of nonmuscle myosin heavy chain II-A in mice. *J. Biol. Chem.* **279**, 41263-41266.
Finnemann, S., Kuhl, M., Otto, G. and Wedlich, D. (1995). Cadherin transfection of Xenopus XTC cells downregulates expression of substrate adhesion molecules. *Mol. Cell. Biol.* **15**, 5082-5091.
Geeves, M. A. and Holmes, K. C. (1999). Structural mechanism of muscle contraction. *Annu. Rev. Biochem.* **68**, 687-728.
Geeves, M. A. and Holmes, K. C. (2005). The molecular mechanism of muscle contraction. *Adv. Protein. Chem.* **71**, 161-193.
Glickman, N. S., Kimmel, C. B., Jones, M. A. and Adams, R. J. (2003). Shaping the zebrafish notochord. *Development* **130**, 873-887.
Golomb, E., Ma, X., Jana, S. S., Preston, Y. A., Kawamoto, S., Shoham, N. G., Goldin, E., Conti, M. A., Sellers, J. R. and Adelstein, R. S. (2004). Identification and characterization of nonmuscle myosin II-C, a new member of the myosin II family. *J. Biol. Chem.* **279**, 2800-2808.

Goto, T. and Keller, R. (2002). The planar cell polarity gene strabismus regulates convergence and extension and neural fold closure in Xenopus. *Dev. Biol.* **247**, 165-181.
Hardin, J. and Keller, R. (1988). The behaviour and function of bottle cells during gastrulation of Xenopus laevis. *Development* **103**, 211-230.
Harris, A. K., Wild, P. and Stopak, D. (1980). Silicone rubber substrata: a new wrinkle in the study of cell locomotion. *Science* **208**, 177-179.
Heisenberg, C. P., Tada, M., Rauch, G. J., Saude, L., Concha, M. L., Geisler, R., Stemple, D. L., Smith, J. C. and Wilson, S. W. (2000). Silberblick/Wnt11 mediates convergent extension movements during zebrafish gastrulation. *Nature* **405**, 76-81.
Holmes, K. C. and Geeves, M. A. (2000). The structural basis of muscle contraction. *Philos. Trans. R. Soc. Lond. B Biol. Sci.* **355**, 419-431.
Iwaki, D. D., Johansen, K. A., Singer, J. B. and Lengyel, J. A. (2001). drumstick, bowl, and lines are required for patterning and cell rearrangement in the Drosophila embryonic hindgut. *Dev. Biol.* **240**, 611-626.
Jaffe, S. H., Friedlander, D. R., Matsuzaki, F., Crossin, K. L., Cunningham, B. A. and Edelman, G. M. (1990). Differential effects of the cytoplasmic domains of cell adhesion molecules on cell aggregation and sorting-out. *Proc. Natl. Acad. Sci. USA* **87**, 3589-3593.
Keller, R. (2002). Shaping the vertebrate body plan by polarized embryonic cell movements. *Science* **298**, 1950-1954.
Keller, R. and Danilchik, M. (1988). Regional expression, pattern and timing of convergence and extension during gastrulation of Xenopus laevis. *Development* **103**, 193-209.
Keller, R. and Shook, D. (2004). Gastrulation in Amphibians. In *Gastrulation: From Cells to Embryo* (ed. C. D. Stern). Cold Spring Harbor, NY: Cold Spring Harbor Laboratory Press.
Keller, R., Cooper, M. S., Danilchik, M., Tibbetts, P. and Wilson, P. A. (1989). Cell intercalation during notochord development in Xenopus laevis. *J. Exp. Zool.* **251**, 134-154.
Keller, R., Shih, J. and Domingo, C. (1992). The patterning and functioning of protrusive activity during convergence and extension of the Xenopus organiser. *Dev. Suppl.*, 81-91.
Keller, R., Davidson, L., Edlund, A., Elul, T., Ezin, M., Shook, D. and Skoglund, P. (2000). Mechanisms of convergence and extension by cell intercalation. *Philos. Trans. R. Soc. Lond. B Biol. Sci.* **355**, 897-922.
Keller, R., Davidson, L. A. and Shook, D. R. (2003). How we are shaped: the biomechanics of gastrulation. *Differentiation* **71**, 171-205.
Keller, R. E. (1976). Vital dye mapping of the gastrula and neurula of Xenopus laevis. II. Prospective areas and morphogenetic movements of the deep layer. *Dev. Biol.* **51**, 118-137.
Keller, R. E. (1981). An experimental analysis of the role of bottle cells and the deep marginal zone in gastrulation of Xenopus laevis. *J. Exp. Zool.* **216**, 81-101.
Keller, R. E. (1984). The cellular basis of gastrulation in *Xenopus laevis*: active, postinvolution convergence and extension by mediolateral interdigitation. *Am. Zool.* **24**, 589-603.
Kelley, C. A., Sellers, J. R., Gard, D. L., Bui, D., Adelstein, R. S. and Baines, I. C. (1996). Xenopus nonmuscle myosin heavy chain isoforms have different subcellular localizations and enzymatic activities. *J. Cell Biol.* **134**, 675-687.
Kintner, C. R. and Melton, D. A. (1987). Expression of Xenopus N-CAM RNA in ectoderm is an early response to neural induction. *Development* **99**, 311-325.
Kolega, J. (1986). Effects of mechanical tension on protrusive activity and microfilament and intermediate filament organization in an epidermal epithelium moving in culture. *J. Cell Biol.* **102**, 1400-1411.
Kolega, J. (1998). Cytoplasmic dynamics of myosin IIA and IIB: spatial 'sorting' of isoforms in locomoting cells. *J. Cell Sci.* **111**, 2085-2095.
Laevsky, G. and Knecht, D. A. (2001). Under-agarose folate chemotaxis of Dictyostelium discoideum amoebae in permissive and mechanically inhibited conditions. *Biotechniques* **31**, 1140-2, 1144, 1146-1149.
Laevsky, G. and Knecht, D. A. (2003). Cross-linking of actin filaments by myosin II is a major contributor to cortical integrity and cell motility in restrictive environments. *J. Cell Sci.* **116**, 3761-3770.
Landsverk, M. L. and Epstein, H. F. (2005). Genetic analysis of myosin II assembly and organization in model organisms. *Cell. Mol. Life Sci.* **62**, 2270-2282.
Lee, C. H. and Gumbiner, B. M. (1995). Disruption of gastrulation movements in Xenopus by a dominant-negative mutant for C-cadherin. *Dev. Biol.* **171**, 363-373.
Lengyel, J. A. and Iwaki, D. D. (2002). It takes guts: the Drosophila hindgut as a model system for organogenesis. *Dev. Biol.* **243**, 1-19.
Litman, P., Amieva, M. R. and Furthmayr, H. (2000). Imaging of dynamic changes of the actin cytoskeleton in microextensions of live NIH3T3 cells with a GFP fusion of the F-actin binding domain of moesin. *BMC Cell Biol.* **1**, 1.
Lo, C. M., Wang, H. B., Dembo, M. and Wang, Y. L. (2000). Cell movement is guided by the rigidity of the substrate. *Biophys. J.* **79**, 144-152.
Lo, C. M., Buxton, D. B., Chua, G. C., Dembo, M., Adelstein, R. S. and Wang, Y. L. (2004). Nonmuscle myosin IIb is involved in the guidance of fibroblast migration. *Mol. Biol. Cell* **15**, 982-989.
Marsden, M. and DeSimone, D. W. (2003). Integrin-ECM interactions regulate cadherin-dependent cell adhesion and are required for convergent extension in Xenopus. *Curr. Biol.* **13**, 1182-1191.
Maupin, P., Phillips, C. L., Adelstein, R. S. and Pollard, T. D. (1994). Differential localization of myosin-II isozymes in human cultured cells and blood cells. *J. Cell Sci.* **107**, 3077-3090.
Myers, D. C., Sepich, D. S. and Solnica-Krezel, L. (2002). Convergence and extension in vertebrate gastrulae: cell movements according to or in search of identity? *Trends Genet.* **18**, 447-455.
Niessen, C. M. and Gumbiner, B. M. (2002). Cadherin-mediated cell sorting not determined by binding or adhesion specificity. *J. Cell Biol.* **156**, 389-399.
Nieuwkoop, P. D. and Faber, J. (1967). Normal table of *Xenopus laevis* (Daudin). Amsterdam: North Holland Publishing.
Ninomiya, H., Elinson, R. P. and Winklbauer, R. (2004). Antero-posterior tissue polarity links mesoderm convergent extension to axial patterning. *Nature* **430**, 364-367.
O'Toole, T. E., Katagiri, Y., Faull, R. J., Peter, K., Tamura, R., Quaranta, V., Loftus, J. C., Shattil, S. J. and Ginsberg, M. H. (1994). Integrin cytoplasmic domains mediate inside-out signal transduction. *J. Cell Biol.* **124**, 1047-1059.
Rayment, I. and Holden, H. M. (1994). The three-dimensional structure of a molecular motor. *Trends Biochem. Sci.* **19**, 129-134.
Rochlin, M. W., Itoh, K., Adelstein, R. S. and Bridgman, P. C. (1995). Localization of myosin II A and B isoforms in cultured neurons. *J. Cell Sci.* **108**, 3661-3670.
Schectman. (1942). The mechanics of amphibian gastrulation. I. Gastrulation-producing interactions between various regions of an anuran egg (*Ityla regila*). *Univ. Calif. Publ. Zool.* **51**, 1-39.
Sepich, D. S., Myers, D. C., Short, R., Topczewski, J., Marlow, F. and Solnica-Krezel, L. (2000). Role of the zebrafish trilobite locus in gastrulation movements of convergence and extension. *Genesis* **27**, 159-173.
Shewan, A. M., Maddugoda, M., Kraemer, A., Stehbens, S. J., Verma, S., Kovacs, E. M. and Yap, A. S. (2005). Myosin 2 is a key Rho kinase target necessary for the local concentration of E-cadherin at cell-cell contacts. *Mol. Biol. Cell* **16**, 4531-4542.
Shih, J. and Keller, R. (1992a). Cell motility driving mediolateral intercalation in explants of Xenopus laevis. *Development* **116**, 901-914.
Shih, J. and Keller, R. (1992b). Patterns of cell motility in the organizer and dorsal mesoderm of Xenopus laevis. *Development* **116**, 915-930.
Skoglund, P. and Keller, R. (2007). Xenopus fibrillin regulates directed convergence and extension. *Dev. Biol.* **301**, 404-416.
Skoglund, P., Dzamba, B., Coffman, C. R., Harris, W. A. and Keller, R. (2006). Xenopus fibrillin is expressed in the organizer and is the earliest component of matrix at the developing notochord-somite boundary. *Dev. Dyn.* **235**, 1974-1983.
Tada, M. and Smith, J. C. (2000). Xwnt11 is a target of Xenopus Brachyury: regulation of gastrulation movements via Dishevelled, but not through the canonical Wnt pathway. *Development* **127**, 2227-2238.
Tao, Q., Nandadasa, S., McCrea, P. D., Heasman, J. and Wylie, C. (2007). G-protein-coupled signals control cortical actin assembly by controlling cadherin expression in the early Xenopus embryo. *Development* **134**, 2651-2661.
Vicente-Manzanares, M., Zareno, J., Whitmore, L., Choi, C. K. and Horwitz, A. F. (2007). Regulation of protrusion, adhesion dynamics, and polarity by myosins IIA and IIB in migrating cells. *J. Cell Biol.* **176**, 573-580.
Winklbauer, R. (1998). Conditions for fibronectin fibril formation in the early Xenopus embryo. *Dev. Dyn.* **212**, 335-345.
Xu, X. S., Kuspa, A., Fuller, D., Loomis, W. F. and Knecht, D. A. (1996). Cell-cell adhesion prevents mutant cells lacking myosin II from penetrating aggregation streams of Dictyostelium. *Dev. Biol.* **175**, 218-226.
Xu, X. S., Lee, E., Chen, T., Kuczmarski, E., Chisholm, R. L. and Knecht, D. A. (2001). During multicellular migration, myosin ii serves a structural role independent of its motor function. *Dev. Biol.* **232**, 255-264.
Zallen, J. A. (2007). Planar polarity and tissue morphogenesis. *Cell* **129**, 1051-1063.
Zallen, J. A. and Wieschaus, E. (2004). Patterned gene expression directs bipolar planar polarity in Drosophila. *Dev. Cell* **6**, 343-355.
Zhong, Y., Brieher, W. M. and Gumbiner, B. M. (1999). Analysis of C-cadherin regulation during tissue morphogenesis with an activating antibody. *J. Cell Biol.* **144**, 351-359.